Vol 15 No 3, March 2006
1009-1963/2006/15(03)/0518-08
Chinese Physics
© 2006 Chin. Phys. Soc.
and IOP Publishing Ltd

# Bursting and spiking due to additional direct and stochastic currents in neuron models*

Yang Zhuo-Qin(杨卓琴)[a)b)†] and Lu Qi-Shao(陆启韶)[a)b)‡]

[a)] *School of Science, Beijing University of Aeronautics and Astronautics, Beijing* 100083, *China*

[b)] *Key Laboratory of Mathematics, Informatics and Behavioral Semantics, Ministry of Education, Beijing* 100083, *China*

(Received 22 October 2004; revised manuscript received 6 September 2005)

Neurons at rest can exhibit diverse firing activities patterns in response to various external deterministic and random stimuli, especially additional currents. In this paper, neuronal firing patterns from bursting to spiking, induced by additional direct and stochastic currents, are explored in rest states corresponding to two values of the parameter $V_{\rm K}$ in the Chay neuron system. Three cases are considered by numerical simulation and fast/slow dynamic analysis, in which only the direct current or the stochastic current exists, or the direct and stochastic currents coexist. Meanwhile, several important bursting patterns in neuronal experiments, such as the period-1 "circle/homoclinic" bursting and the integer multiple "fold/homoclinic" bursting with one spike per burst, as well as the transition from integer multiple bursting to period-1 "circle/homoclinic" bursting and that from stochastic "Hopf/homoclinic" bursting to "Hopf/homoclinic" bursting, are investigated in detail.

**Keywords:** direct current, stochastic current, bursting and spiking, fast/slow dynamic analysis
**PACC:** 0547, 8720

## 1. Introduction

Abundant neuronal firing activities are of fundamental importance to reveal the mechanism of neuronal coding, and many dynamical models have been studied to explore different firing patterns as well as their dynamical behaviours.

Bursting, as a significant firing pattern, was investigated in many experiments[1−4] and theoretical studies,[5−18] and its dynamical behaviour can be described as a transition between a rest state corresponding to a stable equilibrium and a state of repetitive spiking corresponding to a limit cycle attractor.

A systematic theoretical analysis of bursting was pioneered by Rinzel,[5] where it was analysed by separately considering the fast behaviour modulated by the slowly changing parameters. The bursting oscillation is generated as the evolution of the slow variables switches the fast dynamics between steady state and oscillatory state. In the classification scheme first presented in Ref.[6] three types of bursting oscillations were described, i.e. Type I bursting in pancreatic $\beta$-cells,[7] Type II parabolic bursting in neuron $R_{15}$ of the abdominal ganglion of Aplysia,[8] and Type III bursting in cardiac ganglion cells of the lobster.[9]

Many mathematical models of burster can be written in the following singularly perturbed form:[8,11]

$$\dot{x} = f(x, u), \tag{1}$$

$$\dot{u} = \mu g(x, u), \tag{2}$$

where $\mu \ll 1$ represents the ratio of the fast and slow time scales. $x \in \boldsymbol{R}^m$ is the fast variable responsible for repetitive spiking, and $u \in \boldsymbol{R}$ is the slow variable modulating the spiking.

When considering the fast subsystem $\dot{x} = f(x, u)$ and treating the one-dimensional slow variable $u$ as a bifurcation parameter, there are two important bifurcations of the fast subsystem associated with bursting: the bifurcation of a rest state leading to repetitive spiking and that of repetitive spiking leading to a rest state. These two bifurcations of the fast subsystem reveal explicitly how the spike-generating mechanism

*Project supported by the National Natural Science Foundation of China (Grant Nos 10432010 and 10526002).
†E-mail: yangzhuoqin@buaa.edu.cn
‡Corresponding author. E-mail: qishaolu@hotmail.com

interacts with the slow dynamics to produce bursting behaviour and provide a complete classification scheme for periodic fast-slow bursting, see Table 4 in Ref.[11]. In contrast with bursting, periodic repetitive spiking depends on the existence of a large stable limit cycle and always lies near it.

Some authors have had a discussion on the effects of the external stimuli on an individual neuron, caused by various neurotransmitters with excitatory or inhibitory synaptic inputs. A study of Hodgkin–Huxley (HH) neuron under an external sinusoidal stimulus was presented in Ref.[19]. In Ref.[20], the characteristics of the critical amplitude of sinusoidal stimulus in the Morris–Lecar model were investigated numerically. Reference [21] studied the nonlinear firing and signal transduction of a neuron subject to both a constant stimulus and a weak periodic signal. Furthermore, random factors play an important role in firing activities of real neurons. Noise-induced bursting often occurs in excitable neuronal systems owing to the effect of noise on deterministic subthreshold oscillations.[22–27] Investigated in Ref.[28] was the ability of signal detection and transduction of the HH neuronal systems, associated with rhythmic oscillations in the presence of external modulations.

Because neuronal firing patterns are crucial in the neuronal information processing, the dynamical behaviour and transitions of bursting and spiking due to the direct current $I$ and the stochastic current $\xi(t)$, are investigated in the Chay neuron system by using numerical simulation and fast/slow dynamic analysis as a typical example here. This paper is organized as follows. Section 2 presents the Chay model with additional direct and stochastic currents. The distinct processes from bursting to spiking induced by the additional direct and stochastic currents in two rest states for the parameter $V_{\mathrm{K}} = -83\,\mathrm{mV}$ and $-61\,\mathrm{mV}$ are discussed in Sections 3 and 4, respectively. Finally, a conclusion is given in Section 5.

## 2. Chay model with additional direct and stochastic currents

Many neurons or excitable cells possess calcium $Ca^{2+}$-dependent potassium $K^+$ channels and the intracellular calcium concentration regulates the firing patterns via the calcium-dependent potassium channels. The Chay model[12] is a minimal excitable cell model based on a slowly inactivating $Ca^{2+}$ current, and it can simulate many experimental firing patterns of $\beta$-cells, neurons, sensory terminals, neuronal pacemakers and cold receptors, where the calcium-dependent potassium channels play an important role. At the same time, many excitable cells exhibit complex bursting and spiking phenomena in response to various external stimuli. As a consequence, neuronal firing patterns, as well as their dynamical behaviours, are studied here by applying the Chay system with additional direct and stochastic currents.

$$\begin{aligned}\frac{\mathrm{d}V}{\mathrm{d}t} =& g_{\mathrm{I}}^* m_\infty^3 h_\infty (V_{\mathrm{I}} - V) + g_{\mathrm{K,V}}^* (V_{\mathrm{K}} - V) n^4 \\ &+ g_{\mathrm{K,C}}^* \frac{C}{1+C}(V_{\mathrm{K}} - V) \\ &+ g_{\mathrm{L}}^* (V_{\mathrm{I}} - V) + I + \xi(t), \qquad (3)\\ \frac{\mathrm{d}n}{\mathrm{d}t} =& \frac{n_\infty - n}{\tau_n}, \qquad (4)\\ \frac{\mathrm{d}C}{\mathrm{d}t} =& \rho[m_\infty^3 h_\infty (V_{\mathrm{C}} - V) - k_{\mathrm{C}} C], \qquad (5)\end{aligned}$$

where three dynamical variables are $V$ (the membrane potential), $n$ (the probability of opening the voltage-sensitive $K^+$ channel) and $C$ (the intracellular concentration of $Ca^{2+}$ ions). $V_{\mathrm{K}}$ and $V_{\mathrm{C}}$ are the reversal potentials for $K^+$ and $Ca^{2+}$ channels, respectively, and $V_{\mathrm{L}}$ and $V_{\mathrm{I}}$ are those for other ionic channels. The explicit expressions for $m_\infty$, $h_\infty$, $n_\infty$ and $\tau_n$ are the same as those in Ref.[12]. $I$ denotes the direct current, and $\xi(t)$ is the stochastic current with the characteristic of Gaussian white noise (GWN). The statistical properties give $\langle \xi(t) \rangle = 0$ and $\langle \xi(t), \xi(t') \rangle = 2D\delta(t - t')$ where the noise density $D$ is chosen as 0.005 and $\delta(\cdot)$ is the Dirac delta-function. The Chay model is studied for $V_{\mathrm{C}}$ fixed at 336 mV, and both $V_{\mathrm{K}}$ and $I$ being changeable as control parameters. The values of other parameters used here are identical to those in Ref.[12].

In the Chay system, the fast/slow dynamics analysis is used on the basis of the fact that $\rho$ is usually a small quantity, and then $C$ varies much more slowly than the other variables. The fast subsystem (FS) is given by

$$\begin{aligned}\frac{\mathrm{d}V}{\mathrm{d}t} =& g_{\mathrm{I}}^* m_\infty^3 h_\infty (V_{\mathrm{I}} - V) + g_{\mathrm{K,V}}^* (V_{\mathrm{K}} - V) n^4 \\ &+ g_{\mathrm{K,C}}^* \frac{C}{1+C}(V_{\mathrm{K}} - V) \\ &+ g_{\mathrm{L}}^* (V_{\mathrm{I}} - V) + I, \qquad (6)\\ \frac{\mathrm{d}n}{\mathrm{d}t} =& \frac{n_\infty - n}{\tau_n}. \qquad (7)\end{aligned}$$

The nullcline of the slow variable $C$ is given by

$$C = [m_\infty^3(V) h_\infty(V)(V_{\mathrm{C}} - V)]/k_{\mathrm{C}}. \qquad (8)$$

It can be obtained that $V_{\mathrm{K}} \approx -82.386\,\mathrm{mV}$ and $V_{\mathrm{K}} \approx -61.027\,\mathrm{mV}$ are subcritical and supercritical

Hopf bifurcation points of the Chay model without additional currents, respectively. Now consider the effects of the additional direct and stochastic currents in two rest states for two values of $V_K$, i.e. –83 mV and –61 mV, and three cases are discussed as follows: (1) only the direct current exists, i.e. $I \neq 0$ and $\xi(t) = 0$; (2) only the stochastic current exists, i.e. $I = 0$ and $\xi(t) \neq 0$; (3) both the direct and stochastic currents exist, i.e. $I \neq 0$ and $\xi(t) \neq 0$.

# 3. Bursting and spiking due to the additional direct and stochastic currents at the rest state for $V_K = -83$ mV

## 3.1. From period-1 "circle/homoclinic" bursting to repetitive spiking when $I \neq 0$ and $\xi(t) = 0$

When only the direct current $I$ exists for $V_K = -83$ mV, period-1 firing pattern arises and its interspike interval (ISI) turns smaller with the additional direct current $I$ increasing as a bifurcation parameter, which can be seen from the bifurcation diagram constructed by ISI series vs $I$ (see Fig.1).

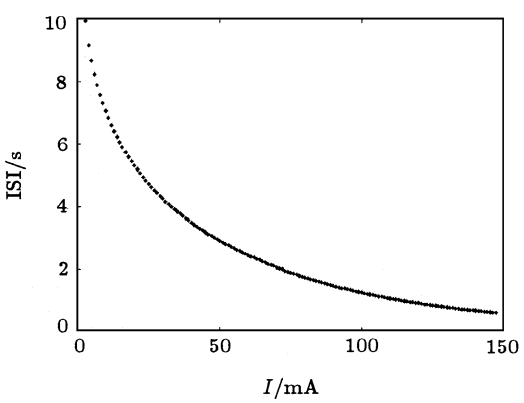



**Fig.1.** Bifurcation diagram constructed by ISI vs the additional direct current $I$ for $V_K = -83$ mV in the Chay model when $I \neq 0$ and $\xi(t) = 0$.

The dynamical behaviour of the period-1 firing pattern induced by the direct current $I$ for $V_K = -83$ mV can be explored by the fast/slow dynamics analysis. Without loss of generality, only period-1 firings for the parameter $I = 70$mA and 100mA will be separately discussed here. The equilibrium points of FS (that is, Eqs.(6) and (7)) with respect to $C$ form the left and the right zigzag curves for these two values of $I$ in the $(C, V)$-phase plane, respectively(see Fig.2(a)). On the upper branch of the curves, the stable foci of FS becoming unstable via the Hopf bifurcations ($H_1$) and ($H_2$), and the stable limit cycles occurring around the unstable focus, are plotted with the maximum and minimum of the membrane potential $V$ (the solid curve). The middle and lower branches are composed of saddles (the dashed curve) and stable nodes (the solid curve), respectively. The nullcline of the slow variable $C$ (the dot-dashed curve) is invariant to $I$, and the equilibrium points of the whole Chay system (3)–(5) for $I = 70$mA and $I = 100$mA are the intersections of the left and the right zigzag curves with the nullcline, respectively. Figure 2(b) is the magnification of the long-dashed rectangular frame in Fig.2(a). Moreover, the trajectories of the period-1 firings for $I = 70$mA and 100mA, respectively, are also appended to Fig.2(b) along with the corresponding left and right zigzag bifurcation curves of FS.

When the direct current $I = 70$mA, the time period of the stable limit cycle of FS grows infinitely for $C = 0.834493 \times 10^{-6}$mol/m$^3$ in Fig.2(c). Furthermore, the stable limit cycle is actually a homoclinic orbit at $C = 0.834493 \times 10^{-6}$mol/m$^3$, in that it passes through the saddle-node point LP1 as shown in Fig.2(d). Therefore, the rest state transits to a spiking state via a saddle-node homoclinic bifurcation (or saddle-node bifurcation on invariant circle) at the point LP1. The trajectory of the system experiences only one spike rather than several spikes, and then hits the middle branch composed of saddles in this spiking process. Therefore, the spiking state disappears via a saddle homoclinic bifurcation, and the trajectory returns to the rest state on the lower branch. Since the rest state disappears via a saddle-node homoclinic bifurcation (or saddle-node bifurcation on invariant circle) and the periodic spiking disappears via a saddle homoclinic orbit bifurcation, the period-1 firing for $I = 70$mA can be classified as the "circle/homoclinic" bursting with one spike per burst.

When the direct current $I = 100$mA, it can also be seen from Fig.2(b) that the trajectory of the system does not hit the middle branch and should actually be repetitive spiking corresponding to a stable limit cycle.

Detailed fast/slow bifurcation analysis confirms that the period-1 firing pattern induced by the direct current $I$ when $V_K = -83$ mV, which fires a spike periodically by all appearances, actually undergoes a slow transition from period-1 "circle/homoclinic" bursting to repetitive spiking about at $I \approx 89.5$mA.

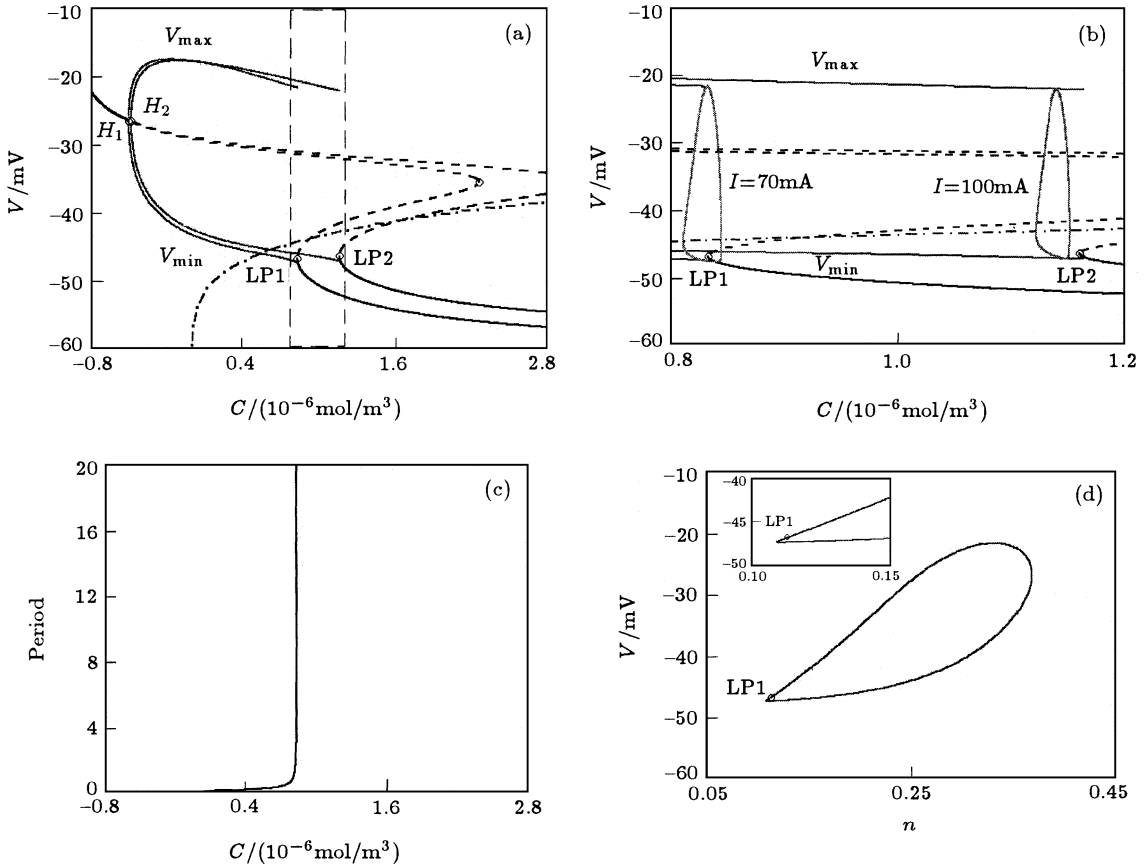



**Fig.2.** Fast/slow dynamics of period-1 firing for $I = 70$mA and 100mA when $V_K = -83$ mV in the Chay model. (a) The bifurcation diagrams of FS with respect to the slow variable $C$ are two zigzag curves. The slow variable's nullcline intersects these two zigzag curves. (b) The magnification of the long-dashed rectangular frame in (a), moreover, the phase portraits of these two period-1 firings are also appended to (b). (c) The period of the stable limit cycle via the Hopf bifurcation with respect to the parameter $C$ for $I = 70$mA. (d) The stable limit cycle passes through the saddle-node point LP1 when $C = 0.834493 \times 10^{-6}$ mol/m$^3$ for $I = 70$mA.

### 3.2. Integer multiple "fold/homoclinic" bursting when $\xi(t) \neq 0$ and $I = 0$

When only the stochastic current $\xi(t)$ exists for $V_K = -83$ mV, integer multiple firing arises as shown in Fig.3, where (a) is the time course of the membrane potential $V$ of the firing pattern and the interspike intervals histogram (ISIH) is shown in (b). It possesses the characteristics: (1) most ISIs are located in integer multiples of a basic ISI; (2) ISIH is multimodal, and the peak decays with ISI increasing.

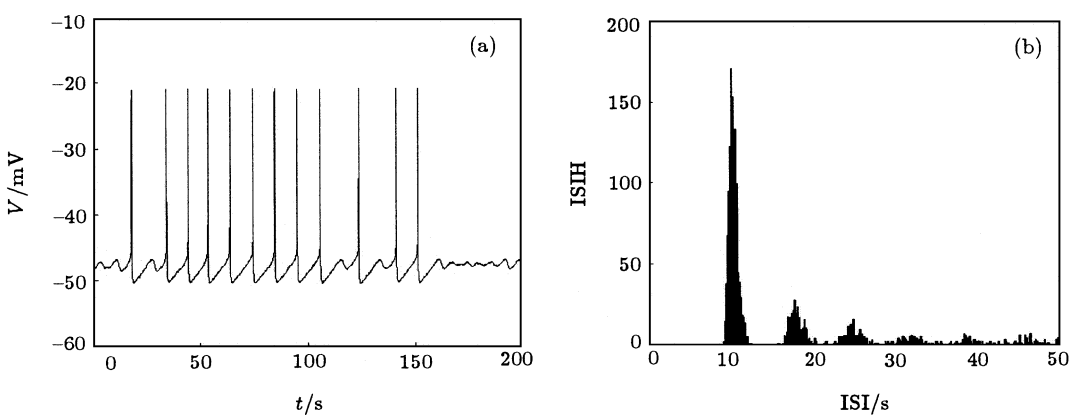



**Fig.3.** The integer multiple firing for $V_K = -83$ mV in the Chay model when $\xi(t) \neq 0$ and $I = 0$: (a) the time evolution of the membrane potential $V$; (b) the interspike interval histogram (ISIH).

Since GWN can be considered as a random combination of uncountable weak independent pulses, the occurrence of GWN-induced integer multiple firing is owing to the response of the corresponding deterministic system to the weak random pulses of GWN.[22,23] The dynamical behaviour of integer multiple firing induced by the stochastic current $\xi(t)$ can be explored by the fast/slow dynamic analysis under the action of weak pulses of GWN as presented in Fig.4.

The bifurcation curve of FS with respect to $C$ is a zigzag curve (see Fig.4(a)). On the upper branch, a stable limit cycle occurs at the point $H$, and the middle and lower branches are composed of saddles and stable nodes, respectively. The trajectory of the integer multiple firing for $V_{\rm K} = -83\,{\rm mV}$ is appended to Fig.4(b), which is the magnification of the long-dashed rectangular frame in Fig.4(a).

It can be seen from the phase portrait of the integer multiple firing in Fig.4(b) that most of the weak pulses provided by GWN only give rise to small amplitude subthreshold oscillations around the stable focus. Subject to certain pulses with proper timing in GWN, however, the trajectory of integer multiple firing can experience a large excursion leading to a spike. Obviously, more emphasis should be focused on this kind of trajectories with large excursions.

In Figs.4(a) and 4(b), the middle and lower branches of the zigzag bifurcation curve of FS coalesce, and a fold bifurcation (off limit cycle) occurs at the point LP1 for $C = 0.34989 \times 10^{-6}{\rm mol/m^3}$, since the saddle-node point (LP1) is situated outside the stable limit cycle for $C = 0.34989 \times 10^{-6}{\rm mol/m^3}$ in Fig.4(c) and the time period of the stable limit cycle tends to infinity when $C = 0.35031 \times 10^{-6}{\rm mol/m^3}$ in Fig.4(d). In this way, the stable rest state on the lower branch disappears via a fold bifurcation at LP1 and transits to a spiking state as the parameter $C$ decreases. The trajectory hits the saddle on the middle branch of the zigzag curve and becomes a homoclinic orbit. Therefore, the spiking state returns to the rest state via a saddle homoclinic bifurcation subsequently.

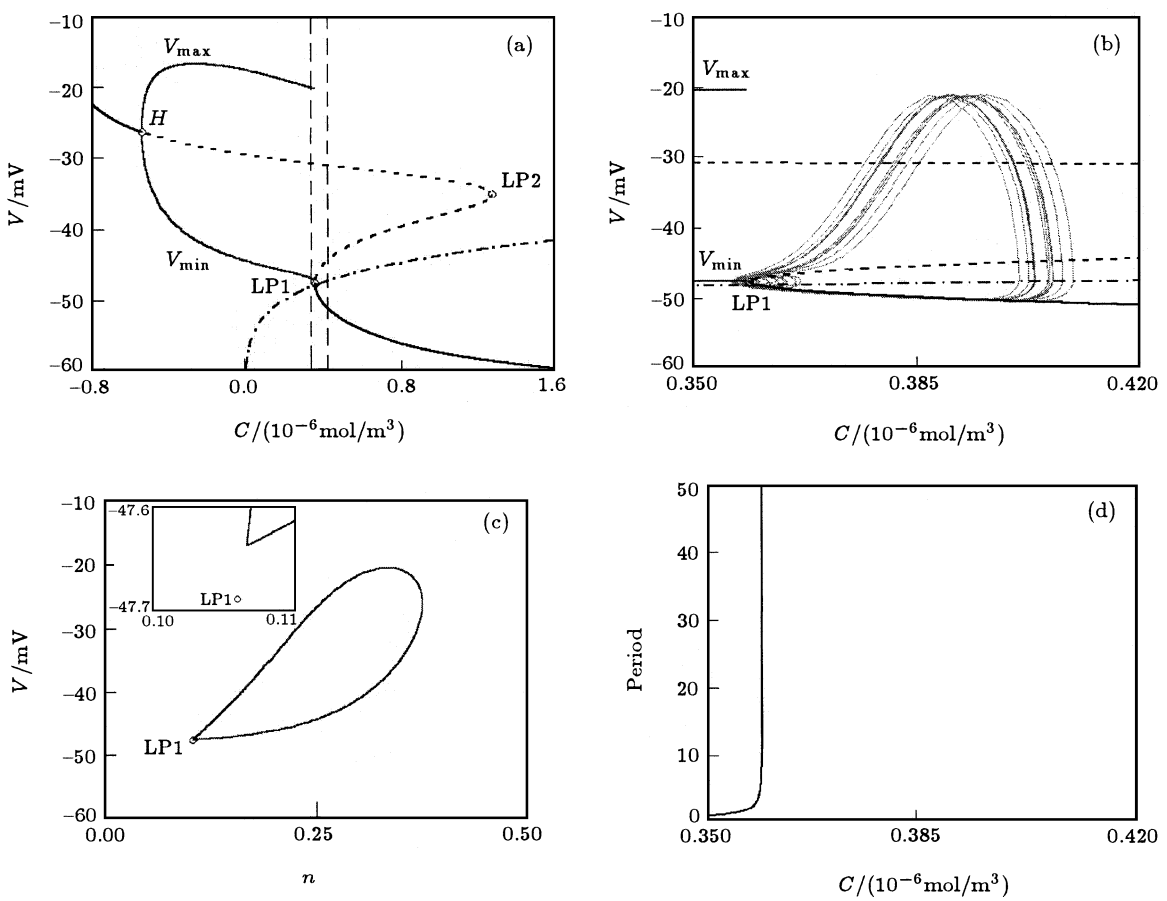



**Fig.4.** (a) The fast/slow dynamics for GWN-induced integer multiple firing when $V_{\rm K} = -83\,{\rm mV}$. (b) The magnification of the long-dashed rectangular frame in (a), where the phase portrait is appended. (c) The stable limit cycle (the red solid curve) and the saddle-node point LP1 for $C = 0.34989 \times 10^{-6}{\rm mol/m^3}$. (d) The period of the stable limit cycle via Hopf bifurcation tending to infinity when $C = 0.35031 \times 10^{-6}{\rm mol/m^3}$.

Nevertheless, whether the trajectory of the system can make large excursions for successive transitions depends on the timing of proper random pulses of GWN, and this means that this process is stochastic. Since in this transition process the rest state disappears via a fold bifurcation and the spiking state disappears via a saddle homoclinic orbit bifurcation, the integer multiple firing is actually the stochastic "fold/homoclinic" bursting with only one spike per burst.

### 3.3. From integer multiple bursting to period-1 "circle/homoclinic" bursting, and to repetitive spiking when $I \neq 0$ and $\xi(t) \neq 0$

When both the direct current and the stochastic current exist for $V_K = -83\,\mathrm{mV}$, it can be seen from the bifurcation diagram constructed by ISI series vs the parameter $I$ in Fig.5 that the Chay system experiences a transition from integer multiple bursting to period-1 "circle/homoclinic" bursting, and to repetitive spiking, and the ISI turns smaller with the additional direct current $I$ increasing.

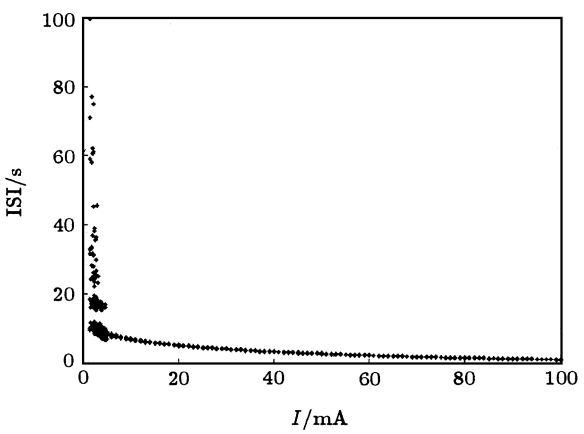



**Fig.5.** Bifurcation diagram of ISI vs the additional direct current $I$ for $V_K = -83\,\mathrm{mV}$ in the Chay model when $I \neq 0$ and $\xi(t) \neq 0$.

## 4. Bursting and spiking due to the additional direct and stochastic currents at the rest state for $V_K = -61\,\mathrm{mV}$

### 4.1. The abrupt transition from periodic "Hopf/homoclinic" bursting to continuous spiking when $I \neq 0$ and $\xi(t) = 0$

When only the direct current exists for $V_K = -61\,\mathrm{mV}$, a distinct bursting is evoked between $I = -65\mathrm{mA}$ and $-56\mathrm{mA}$, and then transits abruptly to continuous spiking as presented in Fig.6 (a), which is completely different from that for $V_K = -83\,\mathrm{mV}$ presented in Section 3.1.

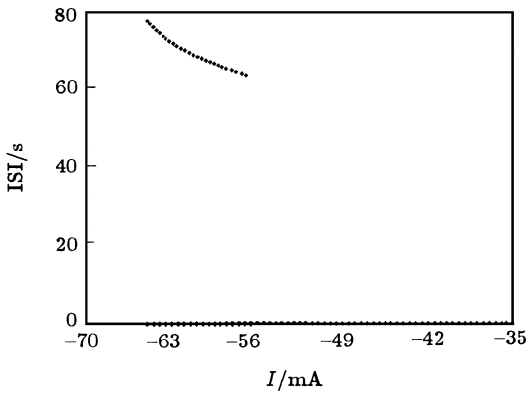



**Fig.6.** Bifurcation diagram of ISI vs the parameter $I$ for $V_K = -61\,\mathrm{mV}$ in the Chay model when $I \neq 0$ and $\xi(t) = 0$.

Consider a typical example of bursting for $I = -60\mathrm{mA}$ in Fig.7(a) by the fast/slow bifurcation analysis in Fig.7(b). The bifurcation diagram of the equilibrium points of FS with respect to the slow variable $C$ consists of an L-shape curve and a parabola-shape curve. The upper and lower branches of the parabola-shape curve, which correspond to saddles (the dashed curve) and stable nodes (the solid curve), respectively, coalesce via a fold bifurcation at the point LP. As $C$ increases, the stable focus (the solid curve) on the L-shape curve becomes unstable (the dashed curve) via a Hopf bifurcation at the point H. At the same time, a stable limit cycle of FS arises around the unstable L-shape curve, and then it meets the saddle on the upper branch of the parabola-shape curve and disappears at $C = 3.63141 \times 10^{-6}\mathrm{mol/m^3}$. The rest states of the whole Chay system (3)–(5) are given by the intersections of the two bifurcation curves with the nullcline of the slow variable $C$ (the dot-dashed curve).

It can be seen from Fig.7(b) that there are two rest states (that is, the up-state and the down-state) appearing in this bursting process, which correspond to the stable foci on the L-shape curve and the stable node on the lower branch of the parabola-shape curve, respectively. The down-state on the parabola-shape curve makes a transition to the up-state on the L-shape curve via a fold bifurcation at the point LP. A small decaying oscillation before the Hopf bifurcation results in the trajectory of bursting converging gradually to the stable focus. And then the up-state disappears, leading to repetitive spiking via a Hopf bifurcation. After several spikes, the repetitive spik-

ing hits the upper branch of the parabola-shape curve composed of saddles. Therefore, the repetitive spiking disappears via a saddle homoclinic bifurcation, and the trajectory of bursting returns again to the down-state on the lower branch of the parabola-shape curve.

Summarily, the down-state transits to the up-state via a fold bifurcation, and the up-state transits to the state of repetitive spiking via a Hopf bifurcation, and repetitive spiking terminates and returns to the down-state via a saddle homoclinic bifurcation. Accordingly, the bursting for $I = -60$mA can be classified as the "Hopf/homoclinic" bursting via a "fold/homoclinic" hysteresis loop.

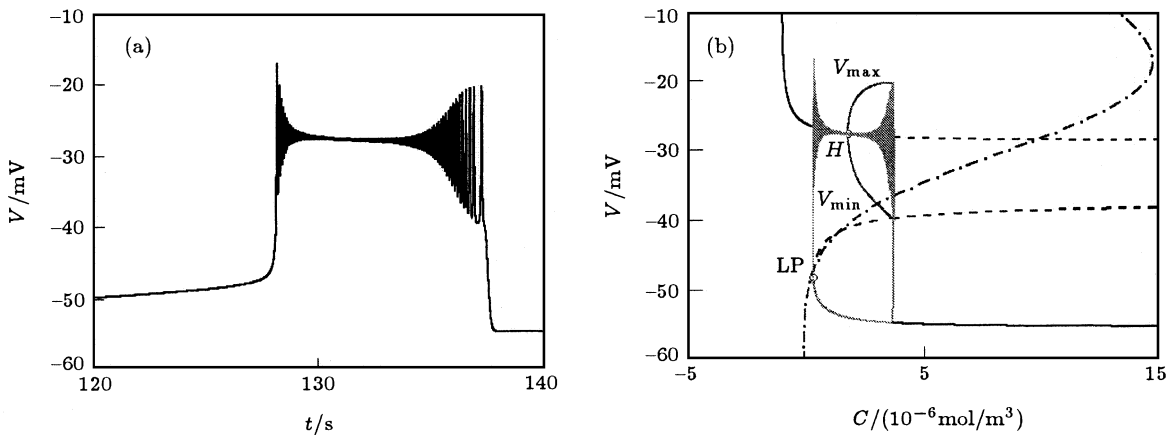



**Fig.7.** The time evolutions of the membrane potential $V$ for the bursting when $I = -60$mA (a) and the fast/slow dynamics analysis on the bursting (b).

### 4.2. Continuous spiking when $\xi(t) \neq 0$ and $I = 0$

When only the stochastic current exists for $V_K = -61$ mV, instead of integer multiple firing, continuous spiking occurs as shown in Fig.8.

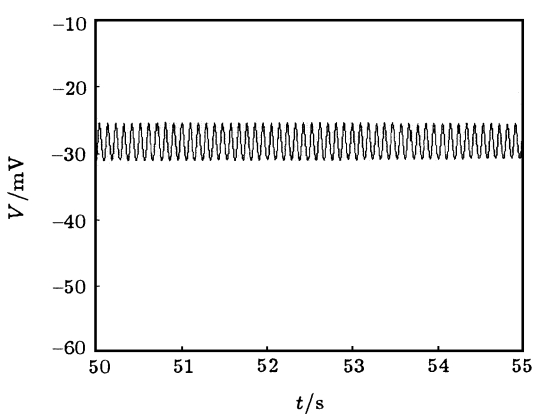



**Fig.8.** The time evolution of continuous spiking for $V_K = -61$ mV when $\xi(t) \neq 0$ and $I = 0$.

### 4.3. From stochastic "Hopf/homoclinic" bursting to periodic "Hopf/homoclinic" bursting to continuous spiking when $I \neq 0$ and $\xi(t) \neq 0$

When both the direct current and the stochastic current exist for $V_K = -61$ mV, it can be seen in Fig.9(a) that the stochastic current expands the range of bursting, which appears between $I = -67$mA and $-49$mA. A transition from stochastic "Hopf/homoclinic" bursting to periodic "Hopf/homoclinic" bursting and then abruptly to continuous spiking is generated in Fig.9(a), and the stochastic "Hopf/homoclinic" bursting for $I = -67$mA is shown in Fig.9(b).

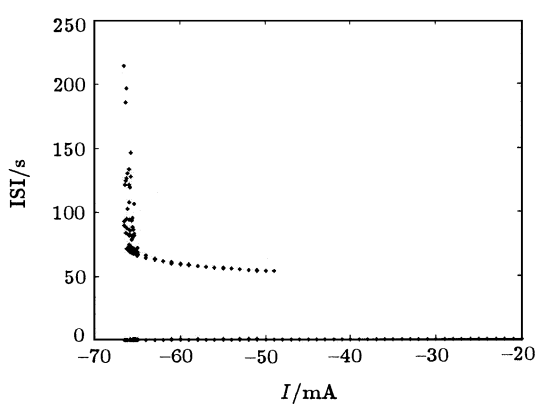



**Fig.9.** (a) Bifurcation diagram of ISI vs the additional direct current $I$ for $V_K = -61$ mV in the Chay model when $I \neq 0$ and $\xi(t) \neq 0$; (b) the stochastic "Hopf/homoclinic" bursting for $I = -67$mA occurring in (a).

## 5. Conclusion

In the neural systems, neurons are always located in an excitatory or inhibitory environment. The effect

of many factors, including fluctuations of synaptic input, dendritic or soma membrane parameters, and so on, can be regarded as an external modulation of the environment to the neurons. Therefore, bursting and spiking due to additional direct current $I$ and stochastic current $\xi(t)$ in the Chay system, as well as their dynamical behaviour, are studied in this paper by numerical simulation and fast/slow dynamic analysis.

Since $V_K \approx -82.386\,\mathrm{mV}$ and $V_K \approx -61.027\,\mathrm{mV}$ are two Hopf bifurcation points in the Chay model without additional currents, the effects of the additional currents are discussed in two rest states near Hopf bifurcations with $V_K$ being –83 mV and –61 mV. Three cases are considered as follows: (1) only the direct current $I$ exists; (2) only the stochastic current $\xi(t)$ exists; (3) the direct current $I$ and the stochastic current $\xi(t)$ coexist.

When only the direct current increases gradually, the firing activity for $V_K = -83\,\mathrm{mV}$ undergoes a slow transition from period-1 "circle/homoclinic" bursting to repetitive spiking, even though it fires a spike periodically by all appearances. When only the stochastic current exists, integer multiple "fold/homoclinic" bursting with one spike per burst occurs and is analysed by fast/slow dynamic analysis with the characteristic of weak pulses of GWN. When both the direct and the stochastic currents exist for $V_K = -83\,\mathrm{mV}$, it can be seen that the Chay system experiences a transition from integer multiple bursting to period-1 "circle/homoclinic" bursting, and then to repetitive spiking. Moreover, ISI turns smaller with the direct current increasing as a bifurcation parameter.

In contrast with the case of $V_K = -83\,\mathrm{mV}$, when only the direct current exists, the firing pattern for $V_K = -61\,\mathrm{mV}$ experiences an abrupt transition from "Hopf/homoclinic" bursting via "fold/homoclinic" hysteresis loop to continuous spiking. However, continuous spiking occurs when only the stochastic current exists. When both the direct and the stochastic currents exist for $V_K = -61\,\mathrm{mV}$, the existence of the stochastic current expands the range of bursting. A transition from stochastic "Hopf/homoclinic" bursting to "Hopf/homoclinic" bursting to continuous spiking can be seen with the direct current increasing.

In conclusion, the induced firing patterns of the Chay model at rest states are distinct and different under the effects of the additional direct and stochastic currents. Since the additional currents are essential for the occurrence of various neuronal firing patterns, the present results about the Chay model are also instructive to the understanding of the complexity in neuronal firing activities in response to abundant external stimuli in neurons other than the Chay model.

## Acknowledgement

The bifurcation diagrams in this paper are obtained by means of the package CONTENT.

## References

[1] Deschenes M, Roy J P and Steriade M 1982 *Brain Res.* **239** 289
[2] Harris-Warrick R M and Flamm R E 1987 *J. Neurosci.* **7** 2113
[3] Ashcroft F and Rorsman P 1989 *Prog. Biophys. Molec. Biol.* **54** 87
[4] Johnson S W, Seutin V and North R A 1992 *Science* **258** 665
[5] Rinzel J 1985 *In: Ordinary and Partial Differential Equations* (Berlin: Springer) p304
[6] Rinzel J 1987 *In: Mathematical Topics in Population Biology, Morphogenesis and Neurosciences* (Berlin: Springer) p267
[7] Sherman A and Rinzel J 1992 *Proc. Natl. Acad. Sci.* USA **89** 2471
[8] Rinzel J and Lee Y S 1987 *J. Math. Biol.* **25** 653
[9] Av-Ron E, Parnas H and Segel L 1993 *Biol. Cybern.* **69** 87
[10] Rush M E and Rinzel J 1994 *Biol. Cybern.* **71** 281
[11] Izhikevich E M 2000 *Int. J. Bif. Chaos* **10** 1171
[12] Chay T R 1985 *Physica* D **16** 233
[13] Kepecs A and Wang X J 2000 *Neurocomputing* **32–33** 81
[14] Soto-Treviño C, Kopell N and Watson D 1996 *J. Math. Biol.* **35** 114
[15] Bertram R, Butte M J, Kiemel T and Sherman A 1995 *Bull. Math. Biol.* **57** 413
[16] Chay T R, Fan Y S and Lee Y S 1995 *Int. J. Bif. Chaos* **5** 595
[17] Booth V, Carr T W and Erneux T 1997 *SIAM J. Applied Math.* **57**(5) 1406
[18] Xie Y, Xu J X, Kang Y M, Hu S J and Duan Y B 2003 *Acta Phys. Sin.* **52** 1112 (in Chinese)
[19] Jin W Y, Xu J X, Wu Y and Hong L 2004 *Chin. Phys.* **13** 335
[20] Xie Y, Xu J X, Kang Y M, Hu S J and Duan Y B 2004 *Chin. Phys.* **13** 1396
[21] Wang W, Wang Y Q and Wang Z D 1998 *Phys. Rev.* E **57** R2527
[22] Balans J P and Casado J M 1998 *Physica* D **122** 231
[23] Longtin A 1997 *Phys. Rev.* E **55** 868
[24] Longtin A 1995 *Chaos* **5** 209
[25] Longtin A and Hinzer K 1996 *Neural Comput.* 8 215
[26] Yang Z Q, Lu Q S, Gu H G and Ren W 2004 *Int. J. Bif. Chaos* **14**(12) 4143
[27] Yang Z Q, Lu Q S, Gu H G and Ren W 2002 *Phys. Lett.* A **299** 499
[28] Yu Y G, Wang W, Wang J F and Liu F 2001 *Phys. Rev.* E **63** 021907